Investigating Markers of Alzheimer's Disease in Posttraumatic Stress Disorder Using Machine Learning and Magnetic Resonance Imaging.

by

Gabriella Yakemow

A Thesis submitted to the Faculty of Graduate Studies of

The University of Manitoba

in partial fulfilment of the requirements of the degree of

MASTER OF SCIENCE

Department of Human Anatomy & Cell Science, Rady Faculty of Health Sciences

University of Manitoba

Winnipeg

Abstract

Introduction: Posttraumatic stress disorder (PTSD) is a mental health disorder caused by experiencing or witnessing traumatic events. Recent studies show that patients with PTSD have an increased risk of developing dementia, including Alzheimer's disease (AD), but there is currently no way to predict which patients will go on to develop AD. The objective of this study was to identify structural and functional neural changes in patients with PTSD that may contribute to the future development of AD.

Methods: Neuroimaging (pseudo-continuous arterial spin labelling [pCASL] and structural magnetic resonance imaging [MRI]) and behavioral data for the current study (n = 67) were taken from our non-randomized, open label clinical trial (ClinicalTrials.gov Identifier: NCT03229915) for treatment-seeking individuals with PTSD (n = 40) and age-matched healthy controls (HC; n = 27). Only the baseline measures were utilized for this study. Mean cerebral blood flow (CBF) and grey matter (GM) volume were compared between groups. Additionally, we utilized two previously established machine learning-based algorithms, one representing AD-like brain activity (Machine learning-based AD Designation [MAD]) and the other focused on AD-like brain structural changes (AD-like Brain Structure [ABS]). MAD scores were calculated from pCASL data and ABS scores were calculated from structural T_1-MRI images. Correlations between neuroimaging data (regional CBF, GM volume, MAD scores, ABS scores) and PTSD symptom severity scores measured by the clinician-administered PTSD scale for DSM-5 (CAPS-5) were assessed.

Results: Decreased CBF was observed in two brain regions (left caudate/striatum and left inferior parietal lobule/middle temporal lobe) in the PTSD group, compared to the HC group. Decreased GM volume was also observed in the PTSD group in the right temporal lobe (parahippocampal gyrus, middle temporal lobe), compared to the HC group. GM volume within the right temporal lobe cluster negatively correlated with CAPS-5 scores and MAD scores in the PTSD group.

Conclusion: Results suggest that patients with PTSD with reduced GM volume in the right temporal regions (parahippocampal gyrus) experienced greater symptom severity and showed more AD-like brain activity. These results show potential for early identification of those who may be at an increased risk for future development of AD.

Acknowledgements

I would like to start by thanking Dr. Ji Hyun Ko for giving me an opportunity to do clinical and novel research in the neuroscience field. Dr. Ko has been a mentor who has pushed me to become a better researcher and never settle for sub-par work. I would like to thank him for allowing me to foster my passion in neuroscience, as well as support me in my future academic goals as I pursue a career in medicine at McMaster University.

Secondly, I would like to acknowledge and thank my committee members Dr. Alexa Hryniuk and Dr. Shaylee Bolton. My journey has not been linear and this project had many pivots I am grateful for your continued support. I would like to especially thank Dr. Sari Hannila, Leilanie Clayton and Jay McMilan for the positive impact you had on my time at the University of Manitoba. Furthermore, I would like to acknowledge the funders I had throughout my research; The University of Manitoba Undergraduate Award, NSERC Indigenous Scholars Award, University of Manitoba Indigenous Scholars Award and the Society for Neuroscience Trainee Professional Development Award.

Lastly, I would like to thank the post-doctoral fellows in my lab, because this project would not have been possible without you! Dr. Tiffany Kolesar was my right-hand throughout this project who read countless drafts and provided immense amounts of mentorship. Dr. Tiffany Carther-Krone who provided comedic relief and a lot of statistical help. Finally, Dr. Iman Beheshti who was always willing to try different and creative ideas while explaining complex topics and encouraging me to continue research in the neuroscience field. I could not have become the researcher I am today without the three of you!

To my family, my mom Pam, dad Byron and, brother Lucas

I could not have finished this without your support throughout this journey.

&

To myself, I did it!

Table of Contents

ABSTRACT 1

ACKNOWLEDGEMENTS 3

LIST OF COPYRIGHTED MATERIAL 8

LIST OF ACRONYMS & ABBREVIATIONS 9

CHAPTER 1- INTRODUCTION 11

CHAPTER 2- BACKGROUND 14

2.1 MAGNETIC RESONANCE IMAGING 14

2.1.1 T_1-weighted Images and Voxel-based Morphometry 16

2.1.2 Pseudo-Continuous Arterial Spin Labeling 17

2.2 POSTTRAUMATIC STRESS DISORDER 18

2.3 ALZHEIMER'S DISEASE 20

2.4 PTSD TO AD PROGRESSION 21

2.5 MACHINE LEARNING ALGORITHMS 22

CHAPTER 3- OBJECTIVES AND HYPOTHESIS 25

3.1- RATIONALE 25

3.2- STUDY OBJECTIVE 25

3.3 – HYPOTHESIS 25

CHAPTER 4- EXPERIMENTAL DESIGN & METHODS 27

4.1 PARTICIPANTS 27

4.2 MRI 28

4.2.1 MRI Sequence Acquisition 28
4.2.2 Structural MRI Analysis 28
4.2.3 CBF Analysis 30
4.3 Machine Learning Calculations: 30
4.3.1 MAD calculation 31
4.3.2 ABS calculation 31
4.4 Statistical Evaluation 33
CHAPTER 5 – RESULTS 34
5.1 Demographic Results 34
5.2 GM Volumes 34
5.3 CBF 34
CHAPTER 6 – DISCUSSION 36
6.1 Demographics 36
6.2 Structural GM 36
6.3 CBF 39
6.4 Limitations 40
6.5- Conclusion/Significance 40
TABLES AND FIGURES: 42
Table 1. Demographic and CAPS-5 data for PTSD and HC groups. 42
Table 2. Whole-brain volume-based morphometry differences between groups (PTSD > HC), using age, sex, and total intracranial volume as covariates. 43

TABLE 3. WHOLE-BRAIN CEREBRAL BLOOD FLOW DIFFERENCES BETWEEN GROUPS (PTSD < HC), USING AGE AND SEX AS COVARIATES. 44

TABLE 4: PARTIAL PEARSON CORRELATION RESULTS FOR CAPS-5 SCORES, GM VOLUME, ACTIVITY, MAD SCORES, AND ABS SCORES 45

TABLE 5. MAD SCORES AND ABS SCORES FOR EACH INDIVIDUAL PARTICIPANT. 47

FIGURE 1. WHOLE-BRAIN VOXEL-BASED MORPHOMETRY RESULTS FOR THE PTSD > HC CONTRAST. 51

FIGURE 2. WHOLE-BRAIN CEREBRAL BLOOD FLOW RESULTS FOR THE PTSD > HC CONTRAST. . 52

FIGURE 3. CORRELATION RESULTS 53

FIGURE 4. THE SCATTER PLOT SHOWING THE ALZHEIMER'S DISEASE (AD)-LIKE BRAIN STRUCTURE IN TEST GROUPS. 54

CHAPTER 7- REFERENCES 55

List of Copyrighted Material

Research is published in Frontiers Neurology

Article Type Original Research

Journal Frontiers in Neurology

Section Dementia and Neurodegenerative Diseases

DOI 10.3389/fneur.2024.1470727

Article ID 1470727

List of Acronyms & Abbreviations

AD	Alzheimer’s Disease
ACC	Accuracy
ADNI	Alzheimer’s Disease Neuroimaging Initiative
ABS	Alzheimer's Disease-like Brain Structure Framework
ASL	Arterial Spin Labeling
AUC	Area Under the Curve
BOLD	Blood Oxygen Level Dependent
BA	Brodmann’s Area
CAPS-5	Clinician-Administered PTSD Scale DSM-5
CBF	Cerebral Blood Flow
CSF	Cerebral Spinal Fluid
DSM-5	Diagnostic and Statistical Manual of Mental Disorders, 5th edition
FWE	Family Wise Error
GM	Gray Matter
HC	Healthy Controls
MAD	Machine learning-based AD Designation
MNI	Montreal Neuroimaging Institute
MRI	Magnetic Resonance Imaging
PET	Positron Emission Tomography
PFC	Prefrontal Cortex
PTSD	Posttraumatic Stress Disorder

pCASL	Pseudo-Continuous Arterial Spin Labeling
RF	Radiofrequency
TBI	Traumatic Brain Injury
TE	Echo Time
TEC	Trauma-Exposed Controls
TNC	Trauma-Naïve Controls
TR	Repetition Time
SPM	Statistical Parameter Mapping
VBM	Voxel-Based Morphometry
WM	White Matter

Chapter 1- Introduction

Posttraumatic stress disorder (PTSD) is a mental health disorder caused by experiencing or witnessing traumatic events that include exposure to actual or threatened death, serious injury, or sexual violence (American Psychiatric Association, 2022;Merians et al., 2023). Symptoms consist of intrusive memories, avoidant behaviors, increased anxiety, and flashbacks (Brewin, 2013;American Psychiatric Association, 2022). A recent study has shown that 63% of Canadians above the age of 18 will likely experience at least one traumatic event and that approximately 7% of Canadians will screen positive for PTSD during their lifetime (Statistics Canada, 2021). Prevalence rates appear similar across the United States (Schein et al., 2021;Raut et al., 2022). This risk of PTSD increases in vulnerable populations including: women (Resnick et al., 1993), military personnel (Yehuda et al., 2015), first responders (Lewis-Schroeder et al., 2018) and health care workers (Carmassi et al., 2020). As the population grows, the impact of PTSD will continue to increase—understanding this disorder and its neurobiological impact will be increasingly important for treatment.

PTSD is categorized as a Trauma- and Stressor-Related Disorder and does not have a clear neurobiological cause; yet, emerging evidence suggests that PTSD predisposes individuals to developing dementia later in life (Yaffe et al., 2009;Monfort and Trehel, 2017;Desmarais et al., 2020;American Psychiatric Association, 2022). In fact, it has been suggested that the increased risk of developing dementia following a PTSD diagnosis is 1.5 to 2-fold compared to people without PTSD (Günak et al., 2020;Song et al., 2020). The increased risk of dementia in PTSD spans a variety of diagnoses including frontotemporal dementia, vascular dementia, and Alzheimer's disease (AD) (Mohlenhoff et al., 2017). The present study focuses on the most

prominent cause of dementia (AD), which accounts for approximately 70% of all dementia cases (Moya-Alvarado et al., 2016).

In contrast to PTSD, which can occur at any age but on average begins in young adulthood to middle-age, AD symptoms typically present at around age 65 (Awada, 2015). The biggest risk factor for developing AD is age—47% of people tested above the age of 85 had probable diagnoses of AD (Evans et al., 1989). PTSD and AD share common symptoms including negative changes in mood and cognition, personality changes, memory difficulties and alterations in arousal or reactivity symptoms (Lancaster et al., 2016;Weller and Budson, 2018). A recent study suggests that PTSD symptom severity is associated with accelerated cognitive decline, a leading symptom of AD (Prieto et al., 2023).

Although the neurobiological underpinnings of PTSD have been difficult to isolate, a recent meta-analysis identified several brain regions that have been shown to have reduced grey matter (GM) volume, including the medial frontal gyrus, posterior cingulate gyrus, hippocampus, amygdala, prefrontal cortex (PFC), and insula (Siehl et al., 2023). Furthermore, significant correlations have been observed between increased PTSD symptom severity and decreased GM volume within the temporal lobe, and most commonly in the hippocampus (Gilbertson et al., 2002;Villarreal et al., 2002;Harnett et al., 2020). Interestingly, AD also typically shows neurodegeneration in the medial temporal lobe, hippocampus and amygdala (Frisoni et al., 2010;Vemuri and Jack, 2010;Deture and Dickson, 2019;de Flores et al., 2022;Kim et al., 2022). In addition to these memory-related brain regions, AD can also be characterized by decreased activity (cerebral blood flow (CBF) or metabolism) in the frontal and posterior cingulate cortex (Syed et al., 1992;Alsop et al., 2000;Roher et al., 2012;Ortner et al., 2019;Thakur and Snekhalatha, 2022) which are also commonly found in PTSD (Schuff et al., 2011;Garip and Ozdemir,

2013;Zandieh et al., 2016;Soncin et al., 2022). These overlapping neuroimaging findings may point to a mechanism for the increased risk of AD following a PTSD diagnosis.

Currently, no biomarkers are available to identify which patients with PTSD will progress to AD. This study explores different neuroimaging modalities to investigate possible neural biomarkers of dementia in a high-risk population. In this study, we characterize GM volume and CBF differences between PTSD and healthy control (HC) groups, then apply two machine learning algorithms across two neuroimaging modalities to estimate AD-like Brain Structure (ABS) scores (Beheshti et al., 2017) and AD-like activity pattern (Machine learning-based AD Designation [MAD]) scores (Katako et al., 2018) in PTSD. MAD scores indicate how similar a patient's brain activity is to AD patterns of brain activity—the higher the score, the greater the similarity. The MAD algorithm was originally trained using fluorodeoxyglucose (FDG) positron emission tomography (PET) data of 94 patients with AD and 111 age-matched HC from the AD Neuroimaging Initiative (ADNI; http://adni.loni.usc.edu/) database. MAD has been shown to be compatible with CBF images derived from perfusion SPECT (Katako et al., 2018) and pCASL data (Wright et al., 2020). Furthermore, MAD scores have been shown to increase over time only in patients with mild cognitive impairment (MCI) who later progress to dementia—MAD scores of patients with stable MCI remained stationary (Beheshti et al., 2022). Finally, MAD scores were also elevated in patients with epilepsy experiencing cognitive decline, compared to cognitively intact patients with epilepsy (He et al., 2023), suggesting its utility in identifying at-risk individuals with comorbidity.

Chapter 2- Background

Machine learning and artificial intelligence are emerging fields of interest and innovation among the medical field. The goal of this study is to investigate PTSD and identify possible neural markers that may indicate an increased risk of developing dementia, using machine learning techniques. To better understand the context of the results, we must first understand the basics of magnetic resonance imaging (MRI), as well as the specific MRI modalities we will be using, following by the disorders themselves.

2.1 Magnetic Resonance Imaging

MRI is a non-invasive imaging technique that is widely used across the clinical and research fields to identify structural and functional abnormities within the human body. Common neural structural abnormalities that can be identified using MRI include tumors, cysts and changes in brain volume. To begin generating an MR image, the subject lies within a strong magnetic field which causes most protons (i.e., hydrogen atoms) in their body to process (rotate and spin) about the applied magnetic field, at a specific frequency (Passingham and Rowe, 2016). Then, radiofrequency (RF) pulses are applied to disrupt this low energy, equilibrium state in a specific manor—the RF pulse 'knocks' protons out of alignment with the external magnetic field and into a higher energy, anti-parallel state (Passingham and Rowe, 2016). Naturally, over time, the protons lose the energy given by the RF pulse, which results in a signal that can be detected by coils in the MR machine. Importantly, different tissues types (GM, white matter [WM], cerebrospinal fluid [CSF], blood, etc.) have different inherent magnetic properties, which affects how long the it takes the protons to 'relax' to the lower energy state, thus allowing researchers to be able to distinguish

between these tissue types (Passingham and Rowe, 2016). Typically, T_1-weighted MRIs are used to visualize and analyze the tissue density of GM, WM, and CSF within the brain.

Functional MRI (fMRI) is a common method used in neuroscience research and clinical neurology as a proxy for measuring brain activity and relies on blood flow. As such, fMRI can be used to identify locations in the brain that process information about sensation, motor control and cognitive functions. The most common and well-known method for identifying blood flow patterns is using the blood oxygen level dependent (BOLD) signal where relative changes in blood flow may indicate neuronal activity. The concept of BOLD is well established by the neurovascular coupling hypothesis which states that rapid increases in CBF correlates with increased neuronal activity (Drew, 2022).

In contrast to this method, another fMRI technique that can non-invasively estimate CBF is arterial spin labeling (ASL) (Petcharunpaisan, 2010;Chen et al., 2015). ASL techniques use RF pulses to invert free water protons at the base of the brain (Ho, 2018). Recent advances pertaining to ASL techniques have begun improving quality and quantitative determination of perfusion data. One of the first methods derived from ASL was continuous ASL(CASL) which applied continuous, low amplitude RF-pulse, although a novel method at the time it is not used anymore because of the low inversion efficiency (Haller et al., 2016). Inversion efficiency is important for being able to quantify perfusion measurements (Maccotta et al., 1997). This disadvantage led to the creating of pulsed ASL(PASL) which applies a pulsed RF, the limitation with PASL is the low signal to noise ratio and is sensitive to tag dispersion (Dolui et al., 2017). Pseudo continuous ASL (pCASL) is a hybrid approach that combines continues ASL (CASL) and pulsed ASL (PASL) advantages (Ho, 2018). In a 2017 study that contrasted these various techniques, pCASL improved the sensitivity of ASL over PASL (Dolui et al., 2017). They also determined that pCASL was able

to show the highest discrimination between healthy control and MCI groups and provided comparable discrimination to positron emission tomography (PET) (Dolui et al., 2017). This is significant because it signifies that pCASL may provide an alternative non-invasive method for determining relative metabolic results without IV injection and can be obtained during typical MR routines.

2.1.1 T_1-weighted Images and Voxel-based Morphometry

The most common way to identify structural abnormalities within the brain using MRI is by using T_1-weighted images. Two important concepts that determine the weighting of an MR image are relaxation times (TR) and echo times (TE). TR refers to the amount of time between successive RF pulses while TE refers to the time between the RF pulse and the when the signal is read. By manipulating these parameters, we can obtain differently weighted images which yield different neurologically relevant data (Passingham and Rowe, 2016). T_1-weighting uses a short TE and a short TR to produce the image (Passingham and Rowe, 2016). The defining characteristics of identifying a T_1-weighted brain image is that the GM will be darker than the WM, making visualization of GM abnormalities easier to see (Passingham and Rowe, 2016). T_1-weighted images will enhance the signal of fatty tissue and suppresses the signal of the water (Kawahara and Nagata, 2021). More specifically, fatty tissue will appear white or bright and fluid will appear dark—in the case of the brain, that will be CSF (Kawahara and Nagata, 2021). For our study, this is important because we want to focus on grey matter changes and identifying any potential loss of GM (possibly indicating atrophy) in PTSD.

In order to analyze brain imaging results and compare them to various groups, wewill be using a specific tool throughout this study called voxel-based morphometry (VBM). VBM allows

me to analyze whole-brain structure in voxel-by voxel comparisons (note: a voxel is essentially a 3D pixel). Using VBM, I will be able to compare GM, WM and CSF between subject groups to identify if there are any volumetric differences, potentially indicating neurodegenerative processes. In order to identify any volumetric changes between PTSD and HC groups, these T_1-weighted images will be pre-processed and analyzed using Statistical Parameter Mapping (SPM, version 12; Welcome Trust Center for Neuroimaging, London, UK: available at: http://www.fil.ion.ucl.ac.uk/spm) and CAT12 (https://neuro-jena.github.io/cat12-help/) software, implemented in MATLB R2022a (Beheshti and Demirel, 2016).

2.1.2 Pseudo-Continuous Arterial Spin Labeling

The imaging sequence pCASL is an emerging, non-invasive MRI technique allowing researchers to investigate CBF patterns, providing information regarding neural functioning. To measure CBF, pCASL uses magnetically-labeled arterial blood water as an endogenous tracer—a train of rapid, short RF pulses is used to label blood water, which then moves throughout the brain (Nezamzadeh et al., 2010;Dolui et al., 2017). As the blood travels further from the RF pulses, the energy begins to decay, and the lower energy magnetic relaxation state is reached in much the same way as general MRI. One limitation to pCASL imaging is that it can only magnetically label arterial blood water and measure CBF patterns (Borogovac and Asllani, 2012;Haller et al., 2016). This limits pCASL from specifically analyzing proteins or other molecules that are common markers in neurological disorders i.e., Tau protein in AD (Chen et al., 2022). Despite this identified limitation, it has also been well established in the neuroimaging field that pCASL and PET are comparable in relation to CBF values and glucose metabolism (Musiek et al., 2012;Verclytte et al., 2016;Dolui et al., 2020). Importantly, an earlier PET study used radioactively labelled water

to estimate CBF directly, which is similar to the method that pCASL is based on (Zimmer and Luxen, 2012). These results are important as they show the direct comparison between PET and pCASL . From a clinical standpoint, these results are encouraging as PET scans are 1) more invasive due to the injection of a radiotracer, and 2) more expensive while pCASL is a safer/more tolerable and less expensive modality for obtaining highly similar data is welcome both for clinical and research purposes. Importantly, it has been shown that pCASL imaging is sensitive to regional alterations in brain function for patients with AD (Dolui et al., 2017). This imaging technique provides a non-invasive way of measuring perfusion patterns; further research is needed in the application of this technique in more patient groups with varying diseases to confirm its specificity and sensitivity. My study will apply pCASL imaging to participants with PTSD, further advancing this research.

2.2 Posttraumatic Stress Disorder

Mental health disorders are categorized and diagnosed using the Diagnostic and Statistical Manual of Mental Disorders, 5th edition (DSM-5). PTSD is typically caused by first-hand involvement of a traumatic event or by witnessing/hearing a traumatic event. Traumatic events can be subjective and vary among person to person, the most common examples of traumatic events include sexual assault/violence, the death of a family member or a close friend and serious injury (O'Donnell et al., 2017;Weathers et al., 2018). PTSD can cause a wide range of symptoms with varying levels of effects on daily life activities. PTSD symptoms are grouped into four clusters: re-experiencing , avoidance, negative cognition and mood, and arousal and reactivity (American Psychiatric Association, 2022). The gold-standard for diagnosing PTSD is the use of the Clinician-Administered PTSD Scale for the (CAPS-5; DSM-5) (Weathers et al., 2018;American Psychiatric

Association, 2022). This scale will be used throughout my study as an objective value to describe a person's symptom severity. More specifically, meeting the diagnostic criteria for PTSD includes experiencing symptoms for longer than one month and having them interfere with daily life tasks and create daily distress (Weathers et al., 2018;American Psychiatric Association, 2022). Currently, it would be very rare for a physician to perform a neuroimaging test (MRI) to identify PTSD markers within the brain. However, PTSD is also characterized by altered brain network functioning(Hinojosa et al., 2024). Common MRI abnormities seen are associated with the anterior cingulate, amygdala, hippocampus, and insula within the brain when compared to age matched healthy controls (Kunimatsu et al., 2020). More specifically, previous research suggests that there is increased perfusion in the region associated with the limbic system in PTSD patients and decreased perfusion in the superior frontal gyrus and parietal and temporal regions (Chung et al., 2006). My study will use a combination of symptom severity and MRI results to interpret PTSD diagnostic factors.

Treatments for PTSD focus on helping the patients manage and cope with the symptoms, restructure their thoughts and change maladaptive beliefs to help patients reduce daily life impact. Common treatments used include psychotherapy (e.g.,Cognitive Behavioral Therapy, Cognitive Processing Therapy, Prolonged exposure and Eye Movevement Desensitization Therapy), medication (antianxiety or antidepressants), or a combination of the two (Schrader and Ross, 2021). There has been a proven success rate of managing symptoms associated with PTSD; however, the neurological impacts on the brain and possible reversal of altered neural functions still need to be further investigated(Hinojosa et al., 2024).

2.3 Alzheimer's Disease

AD is the most common cause of dementia, an age-related disease associated with the decline of memory and cognition (Knopman et al., 2021). AD severity and progression varies between patients (Weller and Budson, 2018;Knopman et al., 2021). Interestingly, clinical manifestations such as memory loss symptoms and neurobiological factors of AD are common methods to categorize/diagnosis AD (Mckhann et al., 2011). However, the only definitive diagnosis is an autopsy which is why AD is a very complicated disease to have a 100% diagnostic confirmation. Common biological markers for AD include increased beta-amyloid plaques and hyperphosphorylated tau protein tangles in the brain (Weller and Budson, 2018). These neurological findings can be identified by using neuroimaging modalities like PET which can be used to tag desired biological proteins like beta-amyloid and tau proteins (Deture and Dickson, 2019). AD can additionally be characterized by decreased CBF in a variety of areas associated with memory, including frontal, posterior cingulate cortex and temporal lobe/hippocampus (Syed et al., 1992;Alsop et al., 2000;Asllani et al., 2008;Roher et al., 2012;Ortner et al., 2019;Thakur and Snekhalatha, 2022). Blood flow changes can also be assessed using pCASL—some common findings using this modality include decreased CBF patterns in the right caudate nucleus, left hippocampus, right parietal grey matter, right corpus collosum and right insula (Wolk and Detre, 2012;Wang et al., 2013;Camargo and Wang, 2021;Duan et al., 2021;Wang et al., 2022). Lastly, the use of MRI to identify structural abnormalities, mainly found in the temporal lobe/hippocampus, have also been used as a diagnostic marker (de Flores et al., 2022). Interestingly, despite neuropathic and clinical features, AD can still be misdiagnosed or undiagnosed (Beach et al., 2012). An improvement in AD diagnostics and the discovery of identifiable risk factors is greatly needed—this need may be filled in the future using machine

learning technology. It is important to state that despite AD being a prominent clinical research topic, the cure for AD remains elusive, and identifying risk factors and patterns is an important area of research for early disease modification and prevention.

2.4 PTSD to AD progression

The progression from PTSD to AD is a emerging area of research due to the increasing number of similarities that are being identified through neuroimaging studies. PTSD is a mental health disease and AD is primarily categorized as a disease of neurodegeneration. However, emerging investigations are identifying the possibility that PTSD predisposes the development of dementia (Yaffe et al., 2009;Monfort and Trehel, 2017;Desmarais et al., 2020). More specifically, this predisposition of PTSD has been suggested that the increased risk of developing dementia is 1.5 to 2-fold (Günak et al., 2020;Song et al., 2020).

While dementia is diagnosed by neurobiological and symptom profiles, PTSD diagnoses are given strictly by psychiatric symptoms as underlying neurobiological sequalae are not clearly defined. Interestingly, studies have shown the patients who have higher symptom severity associated with PTSD were more likely to have high cognitive decline in later ages which is a hallmark characteristic of dementia (Nilaweera et al., 2020;Prieto et al., 2023). Similarities of neurobiology between PTSD and AD are under frequent investigation to aid in better understanding the increasing risk of neurodegenerative diseases.

Neuroimaging studies of PTSD tend to show decreased CBF in the temporal lobe, hippocampus, frontal cortex, posterior cingulate cortex, and most commonly limbic regions which have a cognitive focus of memory (Schuff et al., 2011;Garip and Ozdemir, 2013;Zandieh et al., 2016;Soncin et al., 2022). Neuroimaging studies investigating AD also show decreased CBF in

the temporal regions commonly associated with memory (Desmarais et al., 2020). These results may possibly show another interesting overlap between AD and PTSD because of the overlap in regions associated with memory deficits.

While a cure for dementia remains elusive, identifying those at risk of developing dementia decades in the future is an important area of research—if the average age of developing PTSD and dementia respectively is 25 and 65, there are possibly 4 decades in which disease-preventing or modifying treatments can be utilized to impact disease progression. Unfortunately, to-date, there are no known neurological biomarkers available to identify which patients with PTSD will go on to develop dementia—this knowledge is crucial for developing timely disease-modifying treatments well before dementia onset.

2.5 Machine Learning Algorithms

Recent developments in machine learning have led to important advances in developing biomarkers for differentiating diseases that previously relied too heavily upon subjective interpretation (Katako et al., 2018;Wright et al., 2020;Beheshti et al., 2022;Wright et al., 2022;He et al., 2023). These predictive models may provide a non-invasive way to prognosticate patients and aid in identifying which patients are likely to respond to which intervention. The most common neuroimaging sequence used in machine learning is T_1-weighted MRI (Burgos, 2023) because several features can be extracted, including regional or whole brain volumes, as well as density including GM, WM, CSF and cortical thickness (Rathore et al., 2017;Burgos, 2023). The application of machine learning to T_1-weighted images has mostly been used in aiding the diagnosis of neurodegenerative disease like dementia, or more specifically, AD (Wen et al., 2020;Burgos, 2023). AD is commonly used in machine learning studies as it is easy to highlight

atrophy and neuronal loss which is a common and well-established criterion of neurodegenerative diseases (Burgos, 2023;Odusami et al., 2024).

Recently, our lab developed a MAD algorithm to differentiate those with AD-like brain metabolism from healthy brain metabolism (Katako et al., 2018;Beheshti et al., 2022). The MAD algorithm was originally trained using PET data using 94 patients with AD and 111 age-matched HC from the AD Neuroimaging Initiative database (ADNI; http://adni.loni.usc.edu/)(Katako et al., 2018). MAD scores indicate how similar a patient's brain activity is to AD brain patterns-higher the score, higher the similarity (Katako et al., 2018). Our research has shown the MAD algorithm is sensitive to healthy age-related brain changes and able to objectively distinguish between AD and HC like brain patterns (Katako et al., 2018). Previously, MAD has been applied to pCASL data to obtain AD-like brain activity similarity scores (Katako et al., 2018;Wright et al., 2020). MAD has also been used to assess longitudinal brain metabolic changes in the prodromal stage of AD to monitor progression from MCI (Beheshti et al., 2022). Results demonstrated that increasing MAD scores (AD-like brain metabolism) significantly correlated with patients who had cognitive decline based on mini-mental status examination (Beheshti et al., 2022).

While the MAD algorithm assesses brain activity and its similarity to AD brain function, we will also be investigating brain structure patterns using machine learning. As stated, common machine learning techniques focus on the use of T_1-weighted images to identify structural changes. Therefore, for a more holistic approach, we found it important to not only look at functional machine learning with MAD but pair this with a previously established structural machine learning algorithm (i.e., ABS)(Beheshti et al., 2017). To first replicate the ABS framework, we downloaded baseline structural MRI data of 402 HC and 284 AD participants from the ADNI dataset (https://adni.loni.usc.edu/). The HCs were confirmed to have no cognitive impairment or

neurological disorder as per ADNI criteria. To prevent any bias towards the majority class and lower the false negative rate in the prediction model, we chose 284 healthy controls at random from a group of 402. The ABS score effectively differentiated between AD patients and HCs in the training dataset using the 10-fold cross-validation method, achieving an accuracy of 92%, sensitivity of 89%, and specificity of 95%. Results were consistent on the validation set with an accuracy of 88%, sensitivity of 83%, and specificity of 83%. The novelty of looking at both structural and functional patterns using machine learning algorithms may create a new model for identifying neurodegenerative disease markers in a non-invasive and objective way.

Chapter 3- Objectives and Hypothesis

3.1- Rationale

Currently, no biomarkers are available to identify which patients with PTSD will progress to AD. In this study, we use machine learning across two neuroimaging modalities to identify AD-like patterns of brain activity and structure in PTSD. This study will also allow us to identify which neuroimaging marker may be more effective for identifying AD-like disease progression: GM or CBF. We will also assess symptom severity (CAPS-5) scores and the relationship with GM and CBF to see if any trends arise. Identifying individuals with PTSD at risk for developing later AD will be crucial to ensuring the best outcomes for these patients and reducing the impact of AD in their lives.

3.2- Study Objective

The ***objective*** of this study is to identify key anatomical and activity patterns that may relate to the potential increased risk of AD in patients with PTSD. I will be applying the MAD algorithm on pCASL data and ABS on T_1-weighted structural MRI to measure brain patterns. These results will then be correlated with clinical symptom severity measures (CAPS-5) to identify the correlations that symptom severity has on CBF and structural differences. We will be able to objectively analyze differences in PTSD participants brain patterns compared to HC. To our knowledge, this is the first study to use machine learning to identify those with PTSD who may have AD-like brain patterns, which may predispose them to later AD development.

3.3 – Hypothesis

It has well been documented that PTSD patients have an increased risk at developing dementia compared to those without PTSD (Yaffe et al., 2009;Monfort and Trehel,

2017;Desmarais et al., 2020;Alves de Araujo Junior et al., 2023). Patients with PTSD tend to show reduced GM compared to the HC groups located in the middle temporal lobe and parahippocampal gyrus (Wrocklage et al., 2017;Crombie et al., 2021). Identifying these regions in a patient group younger than the average age of onset of AD may indicate a possible early regional overlap. I ***hypothesised*** that patients with PTSD would show more prevalent neuroimaging markers that are specific to AD, than age-matched HC using MAD and ABS algorithms.

Chapter 4- Experimental Design & Methods

This study uses data from a clinical trial performed by the Ko Lab and applies two different machine learning algorithms to identify AD brain patterns. We will focus on the brain structural and activity markers that could be potentially contributing to the increased risk of AD development among the PTSD population. All participants underwent MRI scans and symptom severity measures (CAPS-5 scores) and met inclusion and exclusion criteria. Prior to this study none of the patients had the diagnosis of AD.

4.1 Participants

A total of 67 participants aged 18-65 were recruited for the open-label, non-randomized parallel clinical trial (ClinicalTrials.gov Identifier: NCT03229915)—only baseline data were used for the present study. Two groups were included in this study: PTSD (n = 40) and HC (n = 27). Patients in the PTSD group were treatment-seeking individuals who had experienced a criterion: A traumatic event. The HC group consisted of trauma-naïve (TNC; n = 15) and trauma-exposed (TEC; n = 12) participants; due to low sample size TEC and TNC groups were pooled. TEC participants met CAPS-5 Criterion A (i.e., exposure to a traumatic event), while obtaining a CAPS-5 total severity score of ≤ 5. Demographic data are provided in Table 1.

Exclusion criteria for all participants included substance dependence not in remission for at least 3 months, uncontrolled bipolar or psychiatric disorder, history of panic attacks, heart disease, respiratory distress, or neurological conditions including traumatic brain injury (TBI), as well as any MRI contraindications (e.g., metal implants or pregnancy). The CAPS-5 interview was administered to all participants to assess PTSD diagnosis and symptom severity (see Table 1). This study was approved by the Biomedical Research Ethics Board of the University of Manitoba and

performed according to regulations. Participants provided written informed consent prior to participating in the study and received an honorarium for their time.

4.2 MRI

4.2.1 MRI Sequence Acquisition

MRI scans were acquired from all participants to investigate brain structure and function. Scans were acquired using a 3 Tesla, 12-channel Siemens MAGNETOM Verio MRI scanner (Erlangen, Germany) at the Kleysen Institute for Advanced Medicine in Winnipeg, Canada. Imaging acquired during each session included an anatomical T_1-weighted scan (MPRAGE sequence; TR/TE/TI = 2300/3.02/900 ms; flip angle = 9°; field view (FOV) = 256 mm x 256 mm with 1.00 mm x 1.00 mm x 1.00 mm resolution; 240 slices), a resting state functional T_2*- weighted scan (scan duration = 11 minutes; results forthcoming elsewhere), and a pseudo-continuous arterial spin labeling scan (pCASL; TR/TE = 4000/12 ms; flip angle = 90°; FOV = 240 mm x 240 mm with 3.8 mm x 3.8 mm x 5 mm resolution; 90 volumes; 20 slices; slice thickness = 5; inter-slice gap = 1mm; labeling time = 2s; post label delay time = 1.2 s; bandwidth = 3 kHz/pixel). M0 images were also acquired (TR/TE = 8000/12 ms) to calibrate the pCASL images.

4.2.2 Structural MRI Analysis

Structural T_1-weighted images were preprocessed using the CAT12.8.2 toolbox (r2170; https://neuro-jena.github.io/cat/index.html) using SPM12 software (version 6909, www.fil.ion.ucl.ac.uk/spm/). First, a robust bias correction was applied to the MRI scans to reduce intensity variations. Then, the scans were segmented into GM, WM, and CSF maps and spatially normalized into Montreal Neurological Institute (MNI) space (voxel size 1.5 mm x 1.5 mm x 1.5 mm) using the DARTEL algorithm. Modulation was applied to keep the volume information

accurate. For VBM analysis, we smoothed the modulated GM images with an 8 mm^3 full-width at half-maximum (FWHM) Gaussian kernel to improve the signal-to-noise ratio.

In order to detect any morphological differences in GM between individuals with PTSD and healthy controls (HC), we conducted a two-sample t-test on the smoothed GM images using SPM12 software. Age, sex, and total intracranial volume (TIV) were included as covariates during the analysis. An explicit mask, comprised of an average of all participant's GM masks, was used to limit search regions inside the GM of the brain. Results are considered significant at a cluster-forming threshold of $p < 0.001$ (uncorrected) and a cluster-level threshold of $p < 0.05$, corrected using family-wise error (FWE). Individual-level mean GM volumes were extracted from the significant clusters for further correlational analyses.

We estimated the previously described ABS scores (Beheshti et al., 2017) utilizing the region-based morphometry feature in CAT12 to obtain whole-brain GM volumes based on the neuromorphometrics atlas (www.neuromorphometrics.com; 136 regions in total), along with subregions of the hippocampus (18 regions) (Winterburn et al., 2013) and the cerebellum (26 regions) (Park et al., 2014). Additionally, cortical thickness (CT) measurements were assessed using the Desikan-Killiany-Tourville (DKT) atlas, which defines 34 regions of interest in each cerebral hemisphere (Desikan et al., 2006). In order to adjust for variations in brain size, the volumes of each subject were normalized by respective TIV. TIV was determined using the CAT12 toolbox (Gaser et al., 2022). Utilizing the aforementioned brain structure-describing information, ABS ranks the most relevant features for classifying AD vs. HC based on a support vector machine (SVM) (Beheshti et al., 2017).

4.2.3 CBF Analysis

For the CBF analysis, pCASL images were preprocessed using the default parameters of the ASLtbx (https://www.cfn.upenn.edu/zewang/ASLtbx.php) (Wang et al., 2008). First, data were realigned, then co-registered to the structural T_1-weighted image, segmented and spatially normalized to standard MNI space (using nonlinear normalization by applying the deformations from the structural CAT12 analysis), and smoothed with an 8 mm^3 FWHM Gaussian kernel, as described previously (Aljuaid et al., 2019). Mean CBF images were produced and contrasted between the groups using SPM12. Age and sex were included as covariates. An explicit mask using the average whole-brain map of all participants was used to limit search regions within the brain. Results are considered significant at a cluster-forming threshold of $p < 0.001$ (uncorrected) and a cluster-level threshold of $p < 0.05$, corrected using FWE. Mean regional CBF values were extracted from significant clusters for further correlational analyses.

The smoothed mean CBF images were further assessed using our previously developed MAD algorithm; available at: https://www.kolabneuro.com/software1 (Katako et al., 2018). In the original work, out of the five different algorithms tested, the SVM with iterative single data algorithm (ISDA) was the best-performing machine (84% sensitivity and 95% specificity) for distinguishing between AD and HC—this algorithm was used in the present study (Katako et al., 2018).

4.3 Machine Learning Calculations:

Two different approaches that quantitates one's "likeness" of their brain to AD are utilized.

4.3.1 MAD calculation

The pre-processed mean CBF images were analyzed by machine learning-based AD designation (MAD) algorithm (Katako et al., 2018). The MAD algorithm was originally trained using fluorodeoxyglucose (FDG) positron emission tomography (PET) data of 94 patients with AD and 111 age-matched HC from the AD Neuroimaging Initiative (ADNI; http://adni.loni.usc.edu/) database. Out of five different algorithms tested, the support vector machine (SVM) with iterative single data algorithm (ISDA) produced the most sensitive and specific performance, which was utilized in this study. MAD scores indicate how similar a patient's brain activity is to AD brain patterns—the higher the score, the greater the similarity. The algorithm that is used throughout this study has a 84% sensitivity and 95% specificity in distinguishing AD vs Healthy controls (HC) (Katako et al., 2018). MAD has also shown to be compatible with CBF images derived from perfusion SPECT (Katako et al., 2018) and pCASL (Wright et al., 2020). MAD has also been applied to assess longitudinal brain metabolic changes in the prodromal stage of AD to monitor disease progression (Beheshti et al., 2022). Results demonstrated that increasing MAD scores (AD-like brain metabolism) significantly correlated with patients who had cognitive decline based on mini-mental status examination (Beheshti et al., 2022).

4.3.2 ABS calculation

The preprocessing was applied in the same fashion as the region-based morphometry analysis in CAT12. In total, 252 structural brain features (i.e., CT measurements, adjusted whole-brain GM volumes, adjusted hippocampal subregions, and cerebellar subregions) were used as input for the AD-like structural pattern framework. In order to diminish the effects of age and sex

on the predicted values, we regressed out the effects of age and sex from the structural brain feature values by referencing the healthy control (HC) group. The dataset was split at random into two cohorts: a training set, made up of 90% of the data (255 healthy controls (HCs) and 255 AD patients), and a validation set, which consisted of 10% of the data including 29 HCs and 29 ADs. Furthermore, the validation set was used to ensure an unbiased estimate of the model's performance on unseen data. The harmonization of data from multiple datasets was achieved using the ComBat technique in MATLAB (Fortin et al., 2018; https://github.com/Jfortin1/ComBatHarmonization).

To build the prediction model, we employed our previously validated AD identification framework, which incorporated a binary genetic algorithm (GA) to identify the best subset of features, as outlined in (Beheshti et al., 2017). The Fisher criterion was integrated into the objective function of the genetic algorithm. GA works by refining a collection of potential feature groups through multiple generations, all based on the idea of natural selection. At first, random sets of chromosomes (i.e., features) are generated, each representing a potential solution. These sets are then evaluated using a fitness function to determine their effectiveness. The GA then uses operations such as combining features from two groups (crossover) and changing features within a group (mutation) to generate new chromosomes (i.e., features). Eventually, the process aims to find the best possible set of features that maximize the distinction between two groups. The parameters of the GA were configured with 50 populations, 200 iterations, a crossover probability of 0.8, and a mutation probability of 0.3. The optimal settings were identified by conducting a 10-fold cross-validation on the training data to achieve the best performance. The classification method used was a standard support vector machine (SVM) algorithm in MATLAB r2020b, specifically using the 'fitcsvm' function with a linear kernel and automatically determined kernel scale. The final prediction model was created using the entire training set and then applied to the

validation set and our test data. The prediction performance on the training and validation sets was assessed through accuracy, sensitivity, and specificity metrics.

As mentioned in the background, the ABS score effectively differentiated between AD patients and HCs in the training dataset using the 10-fold cross-validation method, achieving an accuracy of 92%, sensitivity of 89%, and specificity of 95%. Results were consistent on the validation set with an accuracy of 88%, sensitivity of 83%, and specificity of 83% (Figure 4).

4.4 Statistical Evaluation

Statistical analyses were conducted using the Statistical Package for the Social Sciences (SPSS; IBM Corp., version 27.0, Armonk NY) software. Demographic data were assessed using independent t-test or chi^2, as appropriate (Table 1). Additionally, correlations between neuroimaging data (significant clusters in GM and CBF whole-brain analyses and MAD and ABS scores) and CAPS-5 total severity scores were assessed. Results were considered significant at $p < 0.05$. A list of all MAD and ABS score are presented in Table 4.

Chapter 5 – Results

5.1 Demographic Results

PTSD and HC groups did not significantly differ for age or sex (Table 1). CAPS-5 scores and years of education significantly differed between groups (Table 1)—the PTSD group had higher PTSD symptom severity scores ($t(65) = 17.771$, $p < 0.001$), as expected. Additionally, the PTSD group on average had fewer years of education ($t(65) = 3.556$, $p = 0.001$). Sex, age, and TIV (GM volume analyses only) were used as covariates throughout the study.

5.2 GM Volumes

Reduced volume was observed in the right middle temporal gyrus/parahippocampal gyrus for the PTSD group, compared to the HC group (Table 2; Figure 1). No regions showed significantly larger volume for the PTSD group, compared to the HC group. GM volume of middle temporal gyrus cluster correlated with CAPS-5 total symptom severity scores ($r = -0.461$; $p = 0.005$; Figure 3).

ABS scores did not show any significant difference between the PTSD and HC ($t(65) = 0.831$, $p = 0.409$). Further evaluation using a proportions z-test indicated that 11.1% (3/27) of the HC group and 7.5% (3/40) of the PTSD group were classified as AD-like, resulting in a z-statistic of 0.5077, $p = 0.6116$ (proportional difference = 3.61%, 95% CI = [-10.78%, 18.00%], Cohen's d = 0.1259), indicating no statistically significant difference between the groups.

5.3 CBF

The PTSD group showed significantly lower CBF in two clusters, primarily in the left hemisphere, compared to the HC group (Table 3; Figure 2). The first cluster (3933 voxels) had peak coordinates in the caudate and striatum and extended to the insula, parahippocampal gyrus,

inferior frontal gyrus, limbic lobe and amygdala. The second cluster (4069 voxels) peaked within the middle temporal gyrus and inferior parietal lobule and extend to the pre- and postcentral gyri. There was no significantly increased CBF for the PTSD group, compared to the HC group. The mean CBF values of either cluster did not correlate with CAPS-5 total severity scores.

MAD scores did not significantly differ between groups ($t(65) = 1.376$, p=0.174). At the individual level, five of the PTSD patients showed MAD scores (z-score) higher than 1.96 ($p < 0.05$), compared to none of the HC participants ($\chi^2 = 3.647$, $p = 0.076$). MAD scores correlated with GM volume in the significant middle temporal gyrus cluster identified above ($r = -0.423$; $p = 0.010$; Figure 3). A non-significant trending correlation was also observed between MAD scores and CAPS-5 total severity scores ($r = 0.302$, $p = 0.065$). Other correlational analysis results are summarized in Table 4.

Chapter 6 – Discussion

The goal of the present study was to find a novel non-invasive early neurological marker of AD in PTSD. We used machine learning algorithms (MAD and ABS) paired with neuroimaging and clinical variables to investigate these markers. The combination of these algorithms and PTSD symptom severity scores (CAPS-5) allowed us to identify a significant region of decreased brain volume in PTSD, associated with greater similarity to AD resting brain activity. Interestingly we noticed these markers in a PTSD participant group whose ages are younger than the typical age of diagnosis of AD.

6.1 Demographics

As expected, and consistent with diagnostic criteria, there was a significant difference in CAPS-5 total symptom severity scores between the PTSD group and HC group, indicating increased PTSD symptom severity in the PTSD group (Weathers et al., 2018;2022;American Psychiatric Association, 2022;Bryan et al., 2022). The CAPS-5 total severity scores were used as our primary psychiatric variable throughout the study. Additionally, education significantly differed between groups (Table 1), which is not surprising given that many of the participants in the PTSD group had careers as public safety personnel, typically requiring fewer years of formal education than our HC cohort, which had higher than average years of education.

6.2 Structural GM

Structural neuroimaging results identified one region of significantly reduced GM volume for the PTSD group, compared to the HCs (Figure 1). This middle temporal gyrus cluster included the parahippocampal cortex and Brodmann's areas (BA) 20 and 21 (Table 2). BA 20 is typically associated with processing visual information and memory association while BA 21 is involved in

semantic memory processing, language processing and visual perception (Berti et al., 2023). Taken together, reduced volume within these regions may be associated with the experience of traumatic events and the ability to recall these memories (Kroes et al., 2011;Brewin, 2013), and may be involved in symptoms such as flashbacks and accurate memory retention of traumatic events (Weathers et al., 2018;American Psychiatric Association, 2022). This result of decreased volume in the middle temporal lobe, more specifically the hippocampus and surrounding regions, is a common finding among PTSD structural neuroimaging results (Kitayama et al., 2005;Gianaros et al., 2007;Greenberg et al., 2014).

Interestingly, GM volume within this region was significantly, negatively correlated with CAPS-5 scores—smaller volume in this region was associated with greater symptom severity—a finding corroborated in the literature (Gilbertson et al., 2002;Villarreal et al., 2002). Furthermore, reduced GM volume in the temporal lobe cluster also correlated with MAD scores. In AD, the middle temporal lobe is the first region to begin showing neurodegeneration (de Flores et al., 2022;Xiao et al., 2022), corresponding to the defining symptom of AD: memory deterioration (Kirshner, 2022). Although a causal role cannot be determined by the present study, it may be the case that individuals with reduced volume in this middle temporal region may be more susceptible to developing AD (as well as PTSD). Alternatively, trauma and the effects of PTSD may cause neurodegeneration in this region that increases the risk of dementia later in life. However, it is interesting to note that recently, psychological trauma in an animal model induced GM volume reduction in the hippocampus and globus pallidum (Ruat et al., 2021). Further large-scale longitudinal investigations such as the UK Brain Bank (https://ukbbn.brainsfordementiaresearch.org) and Biofinder (https://biofinder.se/) should be used to shed more light on causality.

Topographically, MAD scores are determined by the overall whole-brain metabolic pattern, which is projected to a hyperplane used to differentiate between AD and HC (Katako et al., 2018). This hyperplane was largely characterized by hypometabolism in temporal regions. Therefore, it is not surprising that the regional GM reduction in the temporal regions observed in the present study correlated with increasing MAD scores in PTSD (Figure 3). While it remains to be seen whether there is any causal relationship between the location of the GM deterioration and AD progression, the lack of significant correlation within the HC group suggests that the medial temporal lobe may be an important region for predicting AD-risk in PTSD.

None of the ABS scores, which focus on AD-like structural patterns, correlated with any other neuroimaging results (GM, CBF, or MAD) or symptom severity (CAPS-5). Although the regional GM deficiency revealed by VBM analysis (Figure 1) spatially overlapped with features used in ABS classification (Figure 4 , it should be noted that it does not constitute that they reflect the same pathology). The local GM difference between HC and PTSD groups was highly localized and it primarily reflects the PTSD-related changes (hence correlated with CAPS-5). On the contrary, ABS scores did not differ between groups. The relatively small regional atrophy in the right middle temporal lobe in our *cognitively healthy* PTSD sample may have not been sufficient to affect ABS scores, which capture the entire brain structural changes associated with AD. Nevertheless, the MAD score was correlated with regional GM changes. This observation is in line with the finding that AD-specific structural changes appear to occur after the functional (and/or vascular) changes (Iturria-Medina et al., 2016).

6.3 CBF

Previously, alterations in CBF have been shown in PTSD, including increased activation in the amygdala (Sartory et al., 2013) and decreased activity in the ventromedial prefrontal cortex and the inferior frontal gyrus (Hayes et al., 2012). Our current results identified decreased CBF within the left caudate and striatum; this large cluster additionally encompassed the inferior frontal gyrus and insula—these findings confirm previous CBF findings of decreased activity in these cortical regions (Shin et al., 1999;Yin et al., 2011;Hayes et al., 2012;Zhe et al., 2016) . Interestingly, research suggests that the insula and inferior frontal gyrus have become target stimulation regions for improving attentional decline in AD (Chou et al., 2020).

The second cluster, showing significantly reduced CBF in the left middle temporal gyri and inferior parietal lobule in the PTSD group corresponds with the frontoparietal network (FPN; also known as the central executive network), a resting state network associated with attention and executive processing. Previous neuroimaging studies showed both increased (Shaw et al., 2002;Nardo et al., 2011;Im et al., 2016) and decreased activity (Shin et al., 1999;Clark et al., 2003;Shin et al., 2004;Weber et al., 2005;Molina et al., 2010) within this region in PTSD. Discrepancy in activity within this region in the literature may be due to several factors: first, whether resting metabolic/CBF or task-related activity are considered, as outline, second, some studies have found reduced activity within the left IPL in the acute stage following traumatic exposure, when exposed to trauma-related (Ke et al., 2016) or fear-learning stimuli (Harnett et al., 2018). In fact, left IPL activity in the acute phase was negatively correlated with symptom severity three months later (Harnett et al., 2018).

The regional CBF did not correlate with MAD scores. Similar to the above interpretation for the lack of significant correlation between regional GM volumes and ABS scores, the reduced

regional CBF, which reflect PTSD-related changes, may have not been sufficient to influence the MAD scores, which reflect the risks of AD. It should also be noted that CBF images are much noisier than GM images, the regional change of which has shown to be correlated with MAD scores.

6.4 Limitations

Limitations of this study include that its design was cross-sectional in nature; longitudinal study is required to confirm if patients with these identified neurological patterns go on to develop dementia, and more specifically, AD. We also acknowledge that there may be a selection bias for the HC groups as many of these participants were recruited by word of mouth and advertisements within the hospital and university settings, which may contribute to the higher years of education observed in this sample.

6.5- Conclusion/Significance

We used MAD scores for assessing AD-associated brain activity changes and ABS for assessing AD-associated brain structural changes. MAD was correlated with GM volume reduction in the medial temporal area which was correlated with PSTD symptom severity measured by CAPS-5. ABS was not correlated with any other measures. Taken together, as symptom severity increases, the brain structure and function become more AD-like, in the PTSD group—it is possible that these individuals who have higher MAD scores may be more susceptible to developing AD in the future. Interestingly the average age of our PTSD sample (i.e., 40.0 years) shows neurodegeneration and commonly, neurodegeneration in AD typically begins around 55 years of age (Ramachandran et al., 2021). Early identification of individuals at an increased risk

for developing dementia later in life is important for implementing disease-modifying preventative care.

In the current study, we used machine learning for early detection of markers associated with AD in PTSD. This study may provide information that will allow for a better understanding of brain structure and function in PTSD and how it may relate to the progression and possible increased risk of AD and dementia. To our knowledge, this is the first study that uses machine learning to assess the defining characteristics of AD within a PTSD population using neuroimaging.

Tables and Figures:

Table 1. Demographic and CAPS-5 data for PTSD and HC groups.

	PTSD	**HC**	***t* or χ^2**	**df**	***p***
N	40	27			
Age (years)	40.0 (± 11.9)	35.4 (± 14.0)	-1.426	65	0.159
Sex (M:F)	14:26	11:16	0.227	1	0.634
Handedness (R:L)	33:6†	24:3	0.247	1	0.619
Education (years)	14.0 (± 2.6)	16.5 (± 3.2)	3.556	65	0.001*
CAPS-5	33.4 (± 9.4)	0.8 (± 1.5)	17.771	65	<0.001*
MAD	-0.516	0.000	1.376	65	0.174
ABS	0.184	0.229	0.831	65	0.409

*Significant at $p < 0.05$. †Data missing for one participant. MAD scores are z-score normalized. CAPS-5: Clinical-administered PTSD scale for the DSM-5; MAD: machine-learning Alzheimer's disease designation; ABS: Alzheimer's disease brain structure.

Table 2. Whole-brain volume-based morphometry differences between groups (PTSD > HC), using age, sex, and total intracranial volume as covariates.

Region	BA	Voxels	*p*-value	*t*-value	*Peak Coordinates* X	Y	Z
Right Middle Temporal Gyrus	20, 21	1155	0.010*	-4.43	39	6	-33

*Significant at $p < 0.05$, FWE corrected for multiple comparisons. BA: Brodmann Area.

Table 3. Whole-brain cerebral blood flow differences between groups (PTSD < HC), using age and sex as covariates.

Region	BA	Voxels	*p*-value	*t*-value	*Peak Coordinates* X	Y	Z
1) Left Caudate/Striatum	13, 45, 47	3933	0.004*	5.06	-8	9	10
2) Left Middle Temporal Gyrus/Inferior Parietal Lobule	7, 39, 40	4069	0.003*	4.45	-48	-75	28

*Significant at $p < 0.05$, FWE corrected for multiple comparisons. BA: Brodmann Area.

Table 4: Partial Pearson correlation results for CAPS-5 scores, GM volume, activity, MAD scores, and ABS scores.

Correlations	***df***	***r*-value**	***p*-value**
PTSD			
CAPS-5 x MTG volume	34	-0.461	0.005*
CAPS-5 x CBF caudate	35	0.053	0.755
CAPS-5 x CBF IPL	35	-0.091	0.592
CAPS-5 x ABS	34	-0.172	0.314
CAPS-5 x MAD	35	0.298	0.074
MTG volume x CBF caudate	34	-0.091	0.598
MTG volume x CBF IPL	34	-0.281	0.097
MTG volume x ABS	34	-0.198	0.240
MTG volume x MAD	34	-0.423	0.010*
CBF caudate x ABS	34	0.042	0.808
CBF caudate x MAD	35	0.139	0.411
CBF IPL x ABS	34	0.113	0.513
CBF IPL x MAD	35	0.217	0.196
ABS x MAD	34	0.163	0.342
HC			
CAPS-5 x MTG volume	21	-0.211	0.333
CAPS-5 x CBF caudate	22	0.097	0.653
CAPS-5 x CBF IPL	22	0.064	0.768

CAPS-5 ABS	21	-0.045	0.840
CAPS-5 x MAD	22	0.184	0.389
MTG volume x CBF caudate	21	0.065	0.768
MTG volume x CBF IPL	21	0.-279	0.197
MTG volume x ABS	22	0.026	0.906
MTG volume x MAD	21	0.049	0.823
CBF caudate x ABS	21	-0.166	0.449
CBF caudate x MAD	22	0.035	0.870
CBF IPL x ABS	21	-0.112	0.610
CBF IPL x MAD	22	-0.162	0.451
ABS x MAD	21	-0.229	0.292

ABS: Alzheimer's disease-like brain structure; CAPS-5: Clinician-administered PTSD scale for DSM-5; CBF: cerebral blood flow; IPL: inferior parietal lobule; MAD: machine-learning based Alzheimer's disease Designation; MTG: middle temporal gyrus. Age, sex, education and total intracranial volume (GM volume only) were used as covariates for the correlation analyses.

Table 5. MAD scores and ABS scores for each individual participant.

Correlations	**MAD scores**	**ABS**
PTSD (n=40)		
	-1.08	0.02
	1.56	0.01
	-1.86	0.00
	-4.92	0.01
	-1.01	0.04
	-0.04	0.00
	0.20	0.05
	-1.91	0.05
	-3.48	0.00
	-1.82	0.00
	-2.50	0.29
	-0.37	0.36
	0.13	0.08
	-1.75	0.36
	2.82	0.18
	-0.01	0.01
	-1.46	0.20
	-2.23	0.01

	-0.92	0.24
	-0.63	0.13
	-1.81	0.10
	0.94	0.02
	0.52	0.36
	-1.75	0.41
	2.25	0.34
	-0.56	0.05
	-0.85	0.78
	2.23	0.29
	1.42	0.20
	1.57	0.36
	2.08	0.06
	1.87	0.24
	0.79	0.04
	-1.68	0.32
	-0.89	0.03
	-1.72	0.08
	-1.82	0.60
	2.09	0.53
	-1.00	0.11
	-2.78	0.36

HC (n=27)

0.06	0.35
0.91	0.03
0.30	0.28
-1.10	0.19
-0.94	0.32
0.02	0.31
0.28	0.41
0.42	0.02
0.24	0.00
-1.57	0.01
-2.24	0.24
1.59	0.04
-1.31	0.30
-0.66	0.31
0.41	0.41
-1.46	0.19
-0.82	0.90
0.95	0.01
-0.34	0.01

	1.72	0.00
	-0.39	0.21
	1.33	0.05
	0.79	0.05
	0.38	0.02
	0.16	0.60
	0.79	0.90
	0.48	0.02

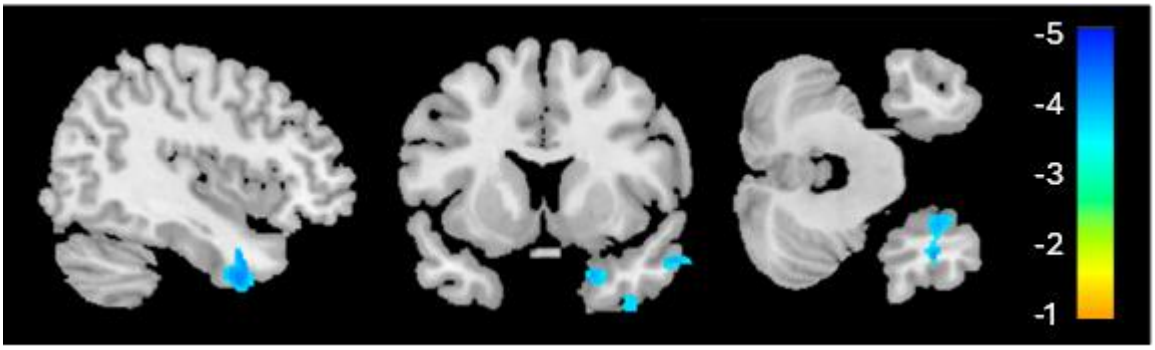

Figure 1. Whole-brain voxel-based morphometry results for the PTSD > HC contrast.

The significant cluster (1155 voxels) is identified in blue, indicating reduced volume in this region for the PTSD group, relative to HC.

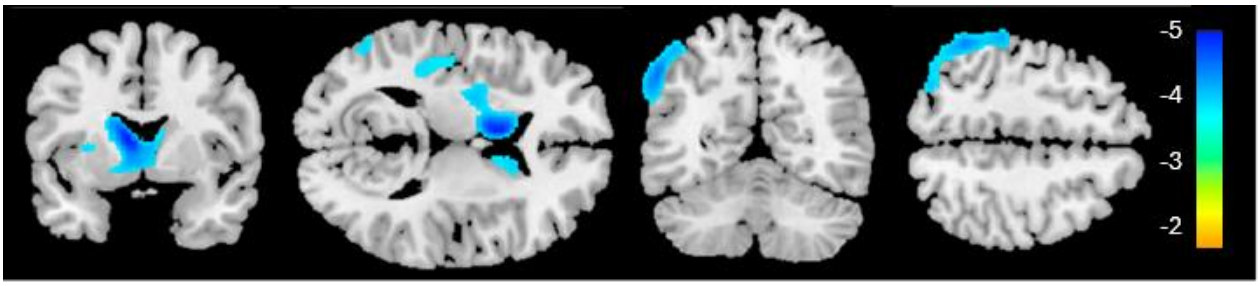

Figure 2. Whole-brain cerebral blood flow results for the PTSD > HC contrast.

Significant clusters are identified in blue, indicating reduced cerebral blood flow in these regions for the PTSD group, relative to HC.

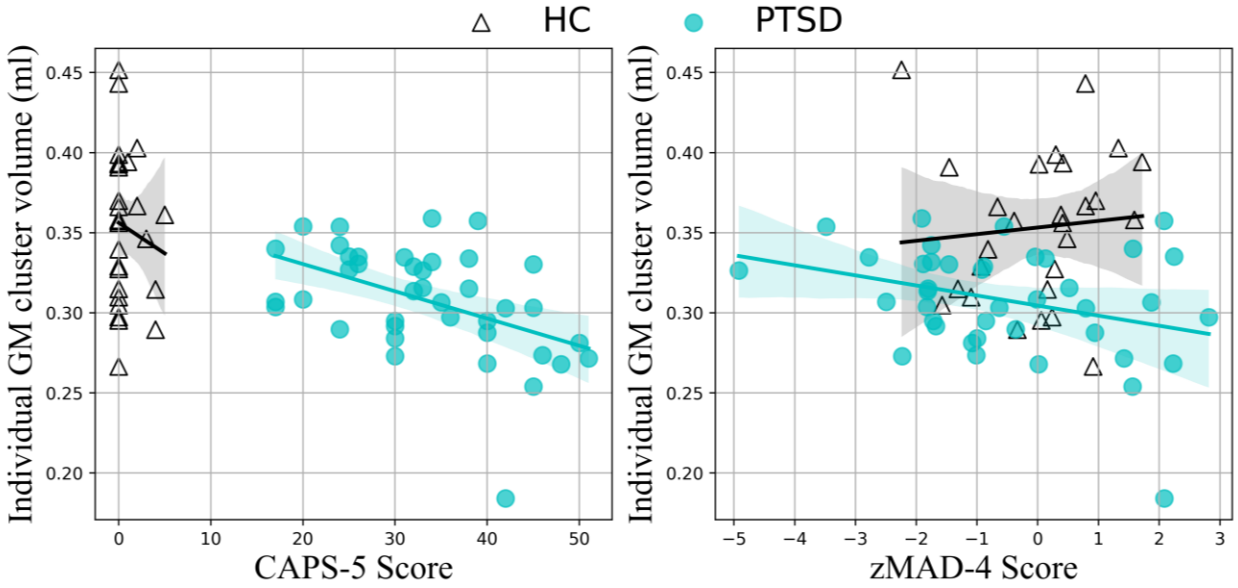

Figure 3**.** Correlation results. Medial temporal lobe volume correlates with CAPS-5 scores (left) and standardized MAD scores (right) in the PTSD group (teal, filled circles), but not the HC group (black, empty triangles).

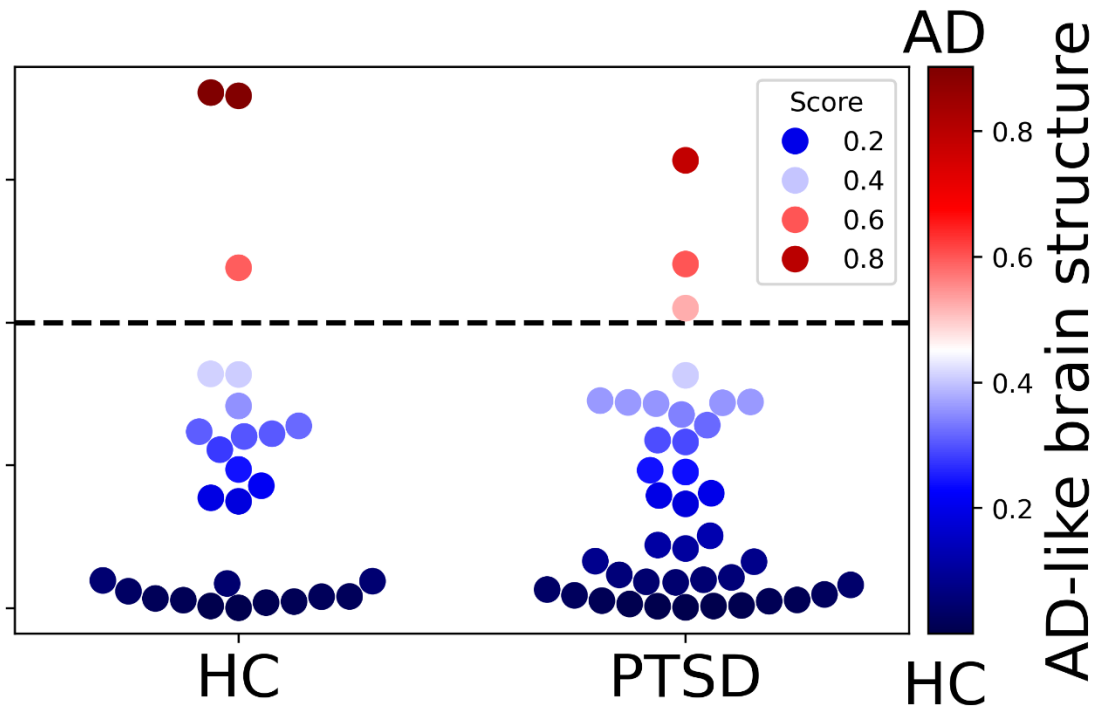

Figure 4. The scatter plot showing the Alzheimer's disease (AD)-like brain structure in test groups. The color bar provides a visual reference for the probability scores, ranging from 0 to 1. A horizontal dashed line at 0.5 denotes the midpoint for reference

Chapter 7- References

(2022). *Diagnostic and statistical manual of mental disorders : DSM-5-TR.* Washington, DC: American Psychiatric Association Publishing.

Aljuaid, M., Booth, S., Hobson, D.E., Borys, A., Williams, K., Katako, A., Ryner, L., Goertzen, A.L., and Ko, J.H. (2019). Blood Flow and Glucose Metabolism Dissociation in the Putamen Is Predictive of Levodopa Induced Dyskinesia in Parkinson's Disease Patients. *Frontiers in neurology* 10**,** 1217-1217.

Alsop, D.C., Detre, J.A., and Grossman, M. (2000). Assessment of cerebral blood flow in Alzheimer's disease by spin-labeled magnetic resonance imaging. *Annals of neurology* 47**,** 93-100.

Alves De Araujo Junior, D., Sair, H.I., Peters, M.E., Carvalho, A.F., Yedavalli, V., Solnes, L.B., and Luna, L.P. (2023). The association between post-traumatic stress disorder (PTSD) and cognitive impairment: A systematic review of neuroimaging findings. *Journal of psychiatric research* 164**,** 259-269.

American Psychiatric Association (2022). *Diagnostic and statistical manual of mental disorders : DSM-5-TR.* Washington, DC: American Psychiatric Association Publishing.

Asllani, I., Habeck, C., Scarmeas, N., Borogovac, A., Brown, T.R., and Stern, Y. (2008). Multivariate and Univariate Analysis of Continuous Arterial Spin Labeling Perfusion MRI in Alzheimer's Disease. *Journal of Cerebral Blood Flow & Metabolism* 28**,** 725-736.

Awada, A.A. (2015). Early and late-onset Alzheimer's disease: What are the differences? *Journal of neurosciences in rural practice* 6**,** 455-456.

Beach, T.G., Monsell, S.E., Phillips, L.E., and Kukull, W. (2012). Accuracy of the Clinical Diagnosis of Alzheimer Disease at National Institute on Aging Alzheimer Disease Centers, 2005–2010. *Journal of Neuropathology & Experimental Neurology* 71**,** 266-273.

Beheshti, I., and Demirel, H. (2016). Feature-ranking-based Alzheimer's disease classification from structural MRI. *Magnetic resonance imaging* 34**,** 252-263.

Beheshti, I., Demirel, H., and Matsuda, H. (2017). Classification of Alzheimer's disease and prediction of mild cognitive impairment-to-Alzheimer's conversion from structural magnetic resource imaging using feature ranking and a genetic algorithm. *Computers in biology and medicine.* 83**,** 109-119.

Beheshti, I., Geddert, N., Perron, J., Gupta, V., Albensi, B.C., and Ko, J.H. (2022). Monitoring Alzheimer's Disease Progression in Mild Cognitive Impairment Stage Using Machine Learning-Based FDG-PET Classification Methods. *Journal of Alzheimer's disease* 89**,** 1493-1502.

Berti, A., Garbarini, F., and Neppi-Modona, M. (2023). "Disorders of higher cortical function," in *Neurobiology of Brain Disorders*. Elsevier), 613-634.

Borogovac, A., and Asllani, I. (2012). Arterial Spin Labeling (ASL) fMRI: Advantages, Theoretical Constrains and Experimental Challenges in Neurosciences. *International Journal of Biomedical Imaging* 2012**,** 1-13.

Brewin, C. (2013). POSTTRAUMATIC STRESS DISORDER AND THE BRAIN. *Journal of neurology, neurosurgery and psychiatry* 84**,** e1-e1.

Bryan, C.J., Russell, H.A., Bryan, A.O., Rozek, D.C., Leifker, F.R., Rugo, K.F., Baker, J.C., Khazem, L.R., Roberge, E.M., Shirley, D.M., and Asnaani, A. (2022). Impact of Treatment Setting and Format on Symptom Severity Following Cognitive Processing Therapy for Posttraumatic Stress Disorder. *Behavior therapy* 53**,** 673-685.

Burgos, N. (2023). "Neuroimaging in Machine Learning for Brain Disorders," in *Neuromethods*. Springer US), 253-284.

Camargo, A., and Wang, Z. (2021). Longitudinal Cerebral Blood Flow Changes in Normal Aging and the Alzheimer's Disease Continuum Identified by Arterial Spin Labeling MRI. *Journal of Alzheimer's disease.* 81**,** 1727-1735.

Carmassi, C., Foghi, C., Dell'oste, V., Cordone, A., Bertelloni, C.A., Bui, E., and Dell'osso, L. (2020). PTSD symptoms in healthcare workers facing the three coronavirus outbreaks: What can we expect after the COVID-19 pandemic. *Psychiatry research* 292**,** 113312-113312.

Chen, J.J., Jann, K., and Wang, D.J.J. (2015). Characterizing Resting-State Brain Function Using Arterial Spin Labeling. *Brain Connectivity* 5**,** 527-542.

Chen, L., Niu, X., Wang, Y., Lv, S., Zhou, X., Yang, Z., and Peng, D. (2022). Plasma tau proteins for the diagnosis of mild cognitive impairment and Alzheimer's disease: A systematic review and meta-analysis. *Frontiers in Aging Neuroscience* 14.

Chou, Y.-H., Ton That, V., and Sundman, M. (2020). A systematic review and meta-analysis of rTMS effects on cognitive enhancement in mild cognitive impairment and Alzheimer's disease. *Neurobiology of Aging* 86**,** 1-10.

Chung, Y.A., Kim, S.H., Chung, S.K., Chae, J.-H., Yang, D.W., Sohn, H.S., and Jeong, J. (2006). Alterations in cerebral perfusion in posttraumatic stress disorder patients without re-exposure to accident-related stimuli. *Clinical neurophysiology* 117**,** 637-642.

Clark, C., Mcfarlane, A.C., Morris, P., Weber, D.L., Sonkkilla, C., Shaw, M., Marcina, J., Tochon-Danguy, H.J., and Egan, G.F. (2003). Cerebral function in posttraumatic stress disorder during verbal working memory updating: a positron emission tomography study. *Biological psychiatry.* 53**,** 474-481.

Crombie, K.M., Ross, M.C., Letkiewicz, A.M., Sartin-Tarm, A., and Cisler, J.M. (2021). Differential relationships of PTSD symptom clusters with cortical thickness and grey matter volumes among women with PTSD. *Scientific Reports* 11.

De Flores, R., Das, S.R., Xie, L., Wisse, L.E.M., Lyu, X., Shah, P., Yushkevich, P.A., and Wolk, D.A. (2022). Medial Temporal Lobe Networks in Alzheimer's Disease: Structural and Molecular Vulnerabilities. *The Journal of neuroscience* 42**,** 2131-2141.

Desikan, R.S., Ségonne, F., Fischl, B., Quinn, B.T., Dickerson, B.C., Blacker, D., Buckner, R.L., Dale, A.M., Maguire, R.P., Hyman, B.T., Albert, M.S., and Killiany, R.J. (2006). An automated labeling system for subdividing the human cerebral cortex on MRI scans into gyral based regions of interest. *Neuroimage* 31**,** 968-980.

Desmarais, P., Weidman, D., Wassef, A., Bruneau, M.-A., Friedland, J., Bajsarowicz, P., Thibodeau, M.-P., Herrmann, N., and Nguyen, Q.D. (2020). The Interplay Between Post-traumatic Stress Disorder and Dementia: A Systematic Review. *The American journal of geriatric psychiatry* 28**,** 48-60.

Deture, M.A., and Dickson, D.W. (2019). The neuropathological diagnosis of Alzheimer's disease. *Molecular Neurodegeneration* 14.

Dolui, S., Li, Z., Nasrallah, I.M., Detre, J.A., and Wolk, D.A. (2020). Arterial spin labeling versus 18F-FDG-PET to identify mild cognitive impairment. *NeuroImage : clinical.* 25**,** 102146.

Dolui, S., Vidorreta, M., Wang, Z., Nasrallah, I.M., Alavi, A., Wolk, D.A., and Detre, J.A. (2017). Comparison of PASL, PCASL, and background-suppressed 3D PCASL in mild cognitive impairment. *Human brain mapping* 38**,** 5260-5273.

Drew, P.J. (2022). Neurovascular coupling: motive unknown. *Trends in neurosciences.* 45**,** 809-819.

Duan, W., Zhou, G.D., Balachandrasekaran, A., Bhumkar, A.B., Boraste, P.B., Becker, J.T., Kuller, L.H., Lopez, O.L., Gach, H.M., and Dai, W. (2021). Cerebral Blood Flow Predicts Conversion of Mild Cognitive Impairment into Alzheimer's Disease and Cognitive Decline: An Arterial Spin Labeling Follow-up Study. *Journal of Alzheimer's disease.* 82**,** 293-305.

Evans, D.A., Funkenstein, H.H., Albert, M.S., Scherr, P.A., Cook, N.R., Chown, M.J., Hebert, L.E., Hennekens, C.H., and Taylor, J.O. (1989). Prevalence of Alzheimer's Disease in a Community Population of Older Persons: Higher Than Previously Reported. *JAMA : the journal of the American Medical Association* 262**,** 2551-2556.

Frisoni, G.B., Fox, N.C., Jack, C.R., Scheltens, P., and Thompson, P.M. (2010). The clinical use of structural MRI in Alzheimer disease. *Nature Reviews Neurology* 6**,** 67-77.

Garip, B., and Ozdemir, B. (2013). 2697 – Reduced glucose metabolism in left lateral parietal cortex of a posttraumatic stress disorder patient: a case report. *European psychiatry* 28**,** 1-1.

Gaser, C., Dahnke, R., Thompson, P.M., Kurth, F., and Luders, E. (2022). CAT-a computational anatomy toolbox for the analysis of structural MRI data. *BioRxiv***,** 2022.2006. 2011.495736.

Gianaros, P.J., Jennings, J.R., Sheu, L.K., Greer, P.J., Kuller, L.H., and Matthews, K.A. (2007). Prospective reports of chronic life stress predict decreased grey matter volume in the hippocampus. *NeuroImage* 35**,** 795-803.

Gilbertson, M.W., Shenton, M.E., Ciszewski, A., Kasai, K., Lasko, N.B., Orr, S.P., and Pitman, R.K. (2002). Smaller hippocampal volume predicts pathologic vulnerability to psychological trauma. *Nature neuroscience* 5**,** 1242-1247.

Greenberg, M.S., Tanev, K., Marin, M.-F., and Pitman, R.K. (2014). Stress, PTSD, and dementia. *Alzheimer's & dementia* 10**,** S155-S165.

Günak, M.M., Billings, J., Carratu, E., Marchant, N.L., Favarato, G., and Orgeta, V. (2020). Post-traumatic stress disorder as a risk factor for dementia: systematic review and meta-analysis. *British journal of psychiatry* 217**,** 600-608.

Haller, S., Zaharchuk, G., Thomas, D.L., Lovblad, K.-O., Barkhof, F., and Golay, X. (2016). Arterial Spin Labeling Perfusion of the Brain: Emerging Clinical Applications. *Radiology* 281**,** 337-356.

Harnett, N.G., Ference, E.W., Wood, K.H., Wheelock, M.D., Knight, A.J., and Knight, D.C. (2018). Trauma exposure acutely alters neural function during Pavlovian fear conditioning. *Cortex* 109**,** 1-13.

Harnett, N.G., Goodman, A.M., and Knight, D.C. (2020). PTSD-related neuroimaging abnormalities in brain function, structure, and biochemistry. *Experimental neurology* 330**,** 113331-113331.

Hayes, J.P., Hayes, S.M., and Mikedis, A.M. (2012). Quantitative meta-analysis of neural activity in posttraumatic stress disorder. *Biology of mood & anxiety disorders* 2**,** 9-9.

He, M., Kolesar, T.A., Goertzen, A.L., Ng, M.C., and Ko, J.H. (2023). Do Epilepsy Patients with Cognitive Impairment Have Alzheimer's Disease-like Brain Metabolism? *Biomedicines* 11**,** 1108.

Hinojosa, C.A., George, G.C., and Ben-Zion, Z. (2024). Neuroimaging of posttraumatic stress disorder in adults and youth: progress over the last decade on three leading questions of the field. *Molecular Psychiatry* 29**,** 3223-3244.

Ho, M.-L. (2018). Arterial spin labeling: Clinical applications. *Journal of neuroradiology. Journal de neuroradiologie.* 45**,** 276-289.

Im, J.J., Namgung, E., Choi, Y., Kim, J.Y., Rhie, S.J., and Yoon, S. (2016). Molecular Neuroimaging in Posttraumatic Stress Disorder. *Experimental Neurobiology* 25**,** 277-295.

Iturria-Medina, Y., Sotero, R.C., Toussaint, P.J., Mateos-Pérez, J.M., Evans, A.C., Weiner, M.W., Aisen, P., Petersen, R., Jack, C.R., Jagust, W., Trojanowki, J.Q., Toga, A.W., Beckett, L., Green, R.C., Saykin, A.J., Morris, J., Shaw, L.M., Khachaturian, Z., Sorensen, G., ..., and Furst, A.J. (2016). Early role of vascular dysregulation on late-onset Alzheimer's disease based on multifactorial data-driven analysis. *Nature Communications* 7**,** 11934.

Katako, A., Shelton, P., Goertzen, A.L., Levin, D., Bybel, B., Aljuaid, M., Yoon, H.J., Kang, D.Y., Kim, S.M., Lee, C.S., and Ko, J.H. (2018). Machine learning identified an Alzheimer's disease-related FDG-PET pattern which is also expressed in Lewy body dementia and Parkinson's disease dementia. *Scientific Reports* 8.

Kawahara, D., and Nagata, Y. (2021). T1-weighted and T2-weighted MRI image synthesis with convolutional generative adversarial networks. *Reports of Practical Oncology and Radiotherapy* 26**,** 35-42.

Ke, J., Zhang, L., Qi, R., Li, W., Hou, C., Zhong, Y., He, Z., Li, L., and Lu, G. (2016). A longitudinal fMRI investigation in acute post-traumatic stress disorder (PTSD). *Acta radiologica.* 57**,** 1387-1395.

Kim, J., Jeong, M., Stiles, W.R., and Choi, H.S. (2022). Neuroimaging Modalities in Alzheimer's Disease: Diagnosis and Clinical Features. *International Journal of Molecular Sciences* 23**,** 6079.

Kirshner, H.S. (2022). Memory Loss, Alzheimer's Disease, and Dementia: A Practical Guide for Clinicians, 3rd ed. *Cognitive and behavioral neurology* 35**,** 298-299.

Kitayama, N., Vaccarino, V., Kutner, M., Weiss, P., and Bremner, J.D. (2005). Magnetic resonance imaging (MRI) measurement of hippocampal volume in posttraumatic stress disorder: A meta-analysis. *Journal of affective disorders* 88**,** 79-86.

Knopman, D.S., Amieva, H., Petersen, R.C., Chételat, G., Holtzman, D.M., Hyman, B.T., Nixon, R.A., and Jones, D.T. (2021). Alzheimer disease. *Nature reviews. Disease primers* 7**,** 33-33.

Kroes, M.C.W., Whalley, M.G., Rugg, M.D., and Brewin, C.R. (2011). Association between flashbacks and structural brain abnormalities in posttraumatic stress disorder. *European psychiatry* 26**,** 525-531.

Kunimatsu, A., Yasaka, K., Akai, H., Kunimatsu, N., and Abe, O. (2020). MRI findings in posttraumatic stress disorder. *Journal of magnetic resonance imaging.* 52**,** 380-396.

Lancaster, C., Teeters, J., Gros, D., and Back, S. (2016). Posttraumatic Stress Disorder: Overview of Evidence-Based Assessment and Treatment. *Journal of Clinical Medicine* 5**,** 105.

Lewis-Schroeder, N.F., Kieran, K., Murphy, B.L., Wolff, J.D., Robinson, M.A., and Kaufman, M.L. (2018). Conceptualization, Assessment, and Treatment of Traumatic Stress in First Responders: A Review of Critical Issues. *Harvard Review of Psychiatry* 26**,** 216-227.

Maccotta, L., Detre, J.A., and Alsop, D.C. (1997). The efficiency of adiabatic inversion for perfusion imaging by arterial spin labeling. *NMR in biomedicine.* 10**,** 216-221.

Mckhann, G.M., Knopman, D.S., Chertkow, H., Hyman, B.T., Jack, C.R., Kawas, C.H., Klunk, W.E., Koroshetz, W.J., Manly, J.J., Mayeux, R., Mohs, R.C., Morris, J.C., Rossor, M.N., Scheltens, P., Carrillo, M.C., Thies, B., Weintraub, S., and Phelps, C.H. (2011). The diagnosis of dementia due to Alzheimer's disease: Recommendations from the National Institute on Aging-Alzheimer's Association workgroups on diagnostic guidelines for Alzheimer's disease. *Alzheimer's & Dementia* 7**,** 263-269.

Merians, A.N., Spiller, T., Harpaz-Rotem, I., Krystal, J.H., and Pietrzak, R.H. (2023). Post-traumatic Stress Disorder. *The medical clinics of North America.* 107**,** 85-99.

Mohlenhoff, B.S., O'donovan, A., Weiner, M.W., and Neylan, T.C. (2017). Dementia Risk in Posttraumatic Stress Disorder: the Relevance of Sleep-Related Abnormalities in Brain Structure, Amyloid, and Inflammation. *Current Psychiatry Reports* 19.

Molina, M.E., Isoardi, R., Prado, M.N., and Bentolila, S. (2010). Basal cerebral glucose distribution in long-term post-traumatic stress disorder. *The World Journal of Biological Psychiatry* 11**,** 493-501.

Monfort, E., and Trehel, G. (2017). Post-traumatic stress disorder secondary to Alzheimer's disease: Emergence of an underlying pathology in the oldest old. *Annales médico psychologiques* 175**,** 776-780.

Moya-Alvarado, G., Gershoni-Emek, N., Perlson, E., and Bronfman, F.C. (2016). Neurodegeneration and Alzheimer's disease (AD). What Can Proteomics Tell Us About the Alzheimer's Brain? *Molecular & cellular proteomics.* 15**,** 409-425.

Musiek, E.S., Chen, Y., Korczykowski, M., Saboury, B., Martinez, P.M., Reddin, J.S., Alavi, A., Kimberg, D.Y., Wolk, D.A., Julin, P., Newberg, A.B., Arnold, S.E., and Detre, J.A. (2012). Direct comparison of fluorodeoxyglucose positron emission tomography and arterial spin labeling magnetic resonance imaging in Alzheimer's disease. *Alzheimer's & Dementia* 8**,** 51-59.

Nardo, D., Högberg, G., Flumeri, F., Jacobsson, H., Larsson, S.A., Hällström, T., and Pagani, M. (2011). Self-rating scales assessing subjective well-being and distress correlate with rCBF in PTSD-sensitive regions. *Psychological medicine.* 41**,** 2549-2561.

Nezamzadeh, M., Matson, G.B., Young, K., Weiner, M.W., and Schuff, N. (2010). Improved pseudo-continuous arterial spin labeling for mapping brain perfusion. *Journal of Magnetic Resonance Imaging* 31**,** 1419-1427.

Nilaweera, D., Freak-Poli, R., Ritchie, K., Chaudieu, I., Ancelin, M.-L., and Ryan, J. (2020). The long-term consequences of trauma and posttraumatic stress disorder symptoms on later life cognitive function and dementia risk. *Psychiatry research.* 294**,** 113506.

O'donnell, M.L., Schaefer, I., Varker, T., Kartal, D., Forbes, D., Bryant, R.A.A., Silove, D., Creamer, M., Mcfarlane, A., Malhi, G., Felmingham, K., Van Hoof, M., Hadzi-Pavlovic, D., Nickerson, A., and Steel, Z. (2017). A systematic review of person-centered approaches to investigating patterns of trauma exposure. *Clinical psychology review.* 57**,** 208-225.

Odusami, M., Maskeliūnas, R., Damaševičius, R., and Misra, S. (2024). Machine learning with multimodal neuroimaging data to classify stages of Alzheimer's disease: a systematic review and meta-analysis. *Cognitive Neurodynamics* 18**,** 775-794.

Ortner, M., Drost, R., Heddderich, D., Goldhardt, O., Müller-Sarnowski, F., Diehl-Schmid, J., Förstl, H., Yakushev, I., and Grimmer, T. (2019). Amyloid PET, FDG-PET or MRI? - the power of different imaging biomarkers to detect progression of early Alzheimer's disease. *BMC Neurology* 19.

Park, M.T.M., Pipitone, J., Baer, L.H., Winterburn, J.L., Shah, Y., Chavez, S., Schira, M.M., Lobaugh, N.J., Lerch, J.P., and Voineskos, A.N. (2014). Derivation of high-resolution MRI atlases of the human cerebellum at 3 T and segmentation using multiple automatically generated templates. *Neuroimage* 95**,** 217-231.

Passingham, R.E., and Rowe, J.B. (2016). *A short guide to brain imaging : the neuroscience of human cognition.* Oxford: Oxford University Press.

Petcharunpaisan, S. (2010). Arterial spin labeling in neuroimaging. *World journal of radiology.* 2**,** 384.

Prieto, S., Nolan, K.E., Moody, J.N., Hayes, S.M., and Hayes, J.P. (2023). Posttraumatic stress symptom severity predicts cognitive decline beyond the effect of Alzheimer's disease biomarkers in Veterans. *Translational Psychiatry* 13.

Ramachandran, A.K., Das, S., Joseph, A., Shenoy, G.G., Alex, A.T., and Mudgal, J. (2021). Neurodegenerative Pathways in Alzheimer's Disease: A Review. *Current neuropharmacology.* 19**,** 679-692.

Rathore, S., Habes, M., Iftikhar, M.A., Shacklett, A., and Davatzikos, C. (2017). A review on neuroimaging-based classification studies and associated feature extraction methods for Alzheimer's disease and its prodromal stages. *NeuroImage* 155**,** 530-548.

Raut, S.B., Marathe, P.A., Van Eijk, L., Eri, R., Ravindran, M., Benedek, D.M., Ursano, R.J., Canales, J.J., and Johnson, L.R. (2022). Diverse therapeutic developments for post-traumatic stress disorder (PTSD) indicate common mechanisms of memory modulation. *Pharmacology & Therapeutics* 239**,** 108195.

Resnick, H.S., Kilpatrick, D.G., Dansky, B.S., Saunders, B.E., and Best, C.L. (1993). Prevalence of Civilian Trauma and Posttraumatic Stress Disorder in a Representative National Sample of Women. *Journal of consulting and clinical psychology* 61**,** 984-991.

Roher, A.E., Debbins, J.P., Malek-Ahmadi, M., Chen, K., Pipe, J.G., Maze, S., Belden, C., Maarouf, C.L., Thiyyagura, P., Mo, H., Hunter, J.M., Kokjohn, T.A., Walker, D.G., Kruchowsky, J.C., Belohlavek, M., Sabbagh, M.N., and Beach, T.G. (2012). Cerebral blood flow in Alzheimer's disease. *Vascular health and risk management* 8**,** 596-611.

Ruat, J., Heinz, D.E., Binder, F.P., Stark, T., Neuner, R., Hartmann, A., Kaplick, P.M., Chen, A., Czisch, M., and Wotjak, C.T. (2021). Structural correlates of trauma-induced hyperarousal in mice. *Progress in neuro-psychopharmacology & biological psychiatry* 111**,** 110404-110404.

Sartory, G., Cwik, J., Knuppertz, H., Schürholt, B., Lebens, M., Seitz, R.J., and Schulze, R. (2013). In Search of the Trauma Memory: A Meta-Analysis of Functional Neuroimaging Studies of Symptom Provocation in Posttraumatic Stress Disorder (PTSD). *PloS one* 8**,** e58150-e58150.

Schein, J., Houle, C., Urganus, A., Cloutier, M., Patterson-Lomba, O., Wang, Y., King, S., Levinson, W., Guérin, A., Lefebvre, P., and Davis, L.L. (2021). Prevalence of post-

traumatic stress disorder in the United States: a systematic literature review. *Current Medical Research and Opinion* 37**,** 2151-2161.

Schrader, C., and Ross, A. (2021). A Review of PTSD and Current Treatment Strategies. *Missouri medicine* 118**,** 546-551.

Schuff, N., Zhang, Y., Zhan, W., Lenoci, M., Ching, C., Boreta, L., Mueller, S.G., Wang, Z., Marmar, C.R., Weiner, M.W., and Neylan, T.C. (2011). Patterns of altered cortical perfusion and diminished subcortical integrity in posttraumatic stress disorder: An MRI study. *NeuroImage* 54**,** S62-S68.

Shaw, M.E., Strother, S.C., Mcfarlane, A.C., Morris, P., Anderson, J., Clark, C.R., and Egan, G.F. (2002). Abnormal Functional Connectivity in Posttraumatic Stress Disorder. *NeuroImage (Orlando, Fla.)* 15**,** 661-674.

Shin, L.M., Mcnally, R.J., Kosslyn, S.M., Thompson, W.L., Rauch, S.L., Alpert, N.M., Metzger, L.J., Lasko, N.B., Orr, S.P., and Pitman, R.K. (1999). Regional Cerebral Blood Flow During Script-Driven Imagery in Childhood Sexual Abuse-Related PTSD: A PET Investigation. *American Journal of Psychiatry* 156**,** 575-584.

Shin, L.M., Orr, S.P., Carson, M.A., Rauch, S.L., Macklin, M.L., Lasko, N.B., Peters, P.M., Metzger, L.J., Dougherty, D.D., Cannistraro, P.A., Alpert, N.M., Fischman, A.J., and Pitman, R.K. (2004). Regional Cerebral Blood Flow in the Amygdala and Medial PrefrontalCortex During Traumatic Imagery in Male and Female Vietnam Veterans With PTSD. *Archives of General Psychiatry* 61**,** 168.

Siehl, S., Zohair, R., Guldner, S., and Nees, F. (2023). Gray matter differences in adults and children with posttraumatic stress disorder: A systematic review and meta-analysis of 113 studies and 11 meta-analyses. *Journal of affective disorders* 333**,** 489-516.

Soncin, L.-D., Faure, S., Mcgonigal, A., Horowitz, T., Belquaid, S., Bartolomei, F., and Guedj, E. (2022). Correlation between FDG-PET brain hypometabolism and PTSD symptoms in temporal lobe epilepsy. *Epilepsia (Copenhagen)*.

Song, H., Sieurin, J., Wirdefeldt, K., Pedersen, N.L., Almqvist, C., Larsson, H., Valdimarsdóttir, U.A., and Fang, F. (2020). Association of Stress-Related Disorders With Subsequent Neurodegenerative Diseases. *JAMA neurology* 77**,** 700-709.

Statistics Canada (2021). *Statistics Canada. Survey on COVID-19 and Mental Health(SCMH)* [Online]. Available: https://www23.statcan.gc.ca/imdb/p2SV.pl?Function=getSurvey&SDDS=5330 [Accessed].

Syed, G.M.S., Eagger, S., O'brien, J., Barrett, J.J., and Levy, R. (1992). Patterns of regional cerebral blood flow in Alzheimer's disease. *Nuclear medicine communications* 13**,** 656-663.

Thakur, M., and Snekhalatha, U. (2022). Multi-stage classification of Alzheimer's disease from 18F-FDG-PET images using deep learning techniques. *Physical and engineering sciences in medicine* 45**,** 1301-1315.

Vemuri, P., and Jack, C.R. (2010). Role of structural MRI in Alzheimer's disease. *Alzheimer's Research & Therapy* 2**,** 23.

Verclytte, S., Lopes, R., Lenfant, P., Rollin, A., Semah, F., Leclerc, X., Pasquier, F., and Delmaire, C. (2016). Cerebral Hypoperfusion and Hypometabolism Detected by Arterial Spin Labeling MRI and FDG-PET in Early-Onset Alzheimer's Disease. *Journal of Neuroimaging* 26**,** 207-212.

Villarreal, G., Hamilton, D.A., Petropoulos, H., Driscoll, I., Rowland, L.M., Griego, J.A., Kodituwakku, P.W., Hart, B.L., Escalona, R., and Brooks, W.M. (2002). Reduced hippocampal volume and total white matter volume in posttraumatic stress disorder. *Biological psychiatry (1969)* 52**,** 119-125.

Wang, X., Wang, D., Li, X., Wang, W., Gao, P., Lou, B., Pfeuffer, J., Zhang, X., Zhu, J., Li, C., and Chen, M. (2022). A diagnostic index based on pseudo-continuous arterial spin labeling and T1-mapping improves efficacy in discriminating Alzheimer's disease from normal cognition. *Frontiers in Neuroscience* 16.

Wang, Z., Aguirre, G.K., Rao, H., Wang, J., Fernández-Seara, M.A., Childress, A.R., and Detre, J.A. (2008). Empirical optimization of ASL data analysis using an ASL data processing toolbox: ASLtbx. *Magnetic resonance imaging* 26**,** 261-269.

Wang, Z., Das, S.R., Xie, S.X., Arnold, S.E., Detre, J.A., and Wolk, D.A. (2013). Arterial spin labeled MRI in prodromal Alzheimer's disease: A multi-site study. *NeuroImage : clinical.* 2**,** 630-636.

Weathers, F.W., Bovin, M.J., Lee, D.J., Sloan, D.M., Schnurr, P.P., Kaloupek, D.G., Keane, T.M., and Marx, B.P. (2018). The Clinician-Administered PTSD Scale for DSM-5 (CAPS-5): Development and Initial Psychometric Evaluation in Military Veterans. *Psychological assessment* 30**,** 383-395.

Weber, D.L., Clark, C.R., Mcfarlane, A.C., Moores, K.A., Morris, P., and Egan, G.F. (2005). Abnormal frontal and parietal activity during working memory updating in post-traumatic stress disorder. *Psychiatry research.* 140**,** 27-44.

Weller, J., and Budson, A. (2018). Current understanding of Alzheimer's disease diagnosis and treatment. *F1000Research* 7**,** 1161.

Wen, J., Thibeau-Sutre, E., Diaz-Melo, M., Samper-González, J., Routier, A., Bottani, S., Dormont, D., Durrleman, S., Burgos, N., and Colliot, O. (2020). Convolutional neural networks for classification of Alzheimer's disease: Overview and reproducible evaluation. *Medical image analysis* 63**,** 101694-101694.

Winterburn, J.L., Pruessner, J.C., Chavez, S., Schira, M.M., Lobaugh, N.J., Voineskos, A.N., and Chakravarty, M.M. (2013). A novel in vivo atlas of human hippocampal subfields using high-resolution 3 T magnetic resonance imaging. *Neuroimage* 74**,** 254-265.

Wolk, D.A., and Detre, J.A. (2012). Arterial spin labeling MRI. *Current Opinion in Neurology* 25**,** 421-428.

Wright, N., Alhindi, A., Millikin, C., Modirrousta, M., Udow, S., Borys, A., Anang, J., Hobson, D.E., and Ko, J.H. (2020). Elevated caudate connectivity in cognitively normal Parkinson's disease patients. *Scientific reports* 10**,** 17978-17978.

Wright, N., Patel, R., Chaulk, S.J., Alcolado, G., Podnar, D., Mota, N., Monson, C.M., Girard, T.A., and Ko, J.H. (2022). Novel Analysis Identifying Functional Connectivity Patterns Associated with Posttraumatic Stress Disorder. *Chronic stress (Thousand Oaks, Calif.)* 6**,** 24705470221092428-24705470221092428.

Wrocklage, K.M., Averill, L.A., Cobb Scott, J., Averill, C.L., Schweinsburg, B., Trejo, M., Roy, A., Weisser, V., Kelly, C., Martini, B., Harpaz-Rotem, I., Southwick, S.M., Krystal, J.H., and Abdallah, C.G. (2017). Cortical thickness reduction in combat exposed U.S. veterans with and without PTSD. *European Neuropsychopharmacology* 27**,** 515-525.

Xiao, S., Yang, Z., Su, T., Gong, J., Huang, L., and Wang, Y. (2022). Functional and structural brain abnormalities in posttraumatic stress disorder: A multimodal meta-analysis of neuroimaging studies. *Journal of psychiatric research* 155**,** 153-162.

Yaffe, K., Vittinghoff, E., Lindquist, K., Barnes, D.E., Covinsky, K.E., Neylan, T., Kluse, M., and Marmar, C. (2009). Post-traumatic stress disorder and risk of dementia among U.S. veterans. *Alzheimer's & dementia* 5**,** P104-P104.

Yehuda, R., Hoge, C.W., Mcfarlane, A.C., Vermetten, E., Lanius, R.A., Nievergelt, C.M., Hobfoll, S.E., Koenen, K.C., Neylan, T.C., and Hyman, S.E. (2015). Post-traumatic stress disorder. *Nature reviews. Disease primers* 1**,** 15057-15057.

Yin, Y., Li, L., Jin, C., Hu, X., Duan, L., Eyler, L.T., Gong, Q., Song, M., Jiang, T., Liao, M., Zhang, Y., and Li, W. (2011). Abnormal baseline brain activity in posttraumatic stress disorder: A resting-state functional magnetic resonance imaging study. *Neuroscience letters* 498**,** 185-189.

Zandieh, S., Bernt, R., Knoll, P., Wenzel, T., Hittmair, K., Haller, J., Hergan, K., and Mirzaei, S. (2016). Analysis of the Metabolic and Structural Brain Changes in Patients with Torture-Related Post-Traumatic Stress Disorder (TR-PTSD) Using 18F-FDG PET and MRI. *Medicine (Baltimore)* 95**,** e3387-e3387.

Zhe, X., Liu, K., Mu, Y.-F., Qi, S., Xi, Y.-B., Du, P., Huan, Y., Tan, Q.-R., Yin, H., Zhao, H.-T., Ge, Y.-L., and Chang, Y.-J. (2016). Decreased Regional Cerebral Perfusion at Resting State in Acute Posttraumatic Stress Disorder Resulting From a Single, Prolonged Stress Event. *Academic radiology.* 23**,** 1083-1090.

Zimmer, L., and Luxen, A. (2012). PET radiotracers for molecular imaging in the brain: Past, present and future. *NeuroImage.* 61**,** 363-370.